

Novel Sliding/Frictional Connections for Improved Seismic Performance of Gypsum Wallboard Partitions

G. Araya-Letelier

Stanford University, USA

Adolfo Ibáñez University, Chile

E. Miranda

Stanford University, USA



SUMMARY:

Non-structural components typically represent between 65% and 85% of the construction cost of commercial buildings, therefore improving the seismic performance of non-structural components can lead to important reductions in the economic impact of earthquakes. Gypsum wallboard partitions are one of the most ubiquitous forms of construction for interior wall partitions. Unfortunately, gypsum partitions are characterized by little deformability, experiencing damage requiring repairs at story drifts ratios (SDR) as low as 0.1%, which leads to important economic losses, downtime and environmental impacts.

To mitigate this damage and the resulting impacts, a new sliding/frictional connection was developed to improve the seismic performance of gypsum partitions. Two full-scale specimens were tested under cyclic reversal loading. One had conventional partitions, whereas the other incorporated the new connection. While the conventional specimen exhibited the first visible damage at a SDR of 0.1%, the specimen with the sliding/frictional connection was damage-free until 1.52%.

Keywords: Non-structural components, gypsum partition walls, loss reduction

1. INTRODUCTION

The cost of non-structural components in commercial buildings is typically considerably larger than the cost of the structure. Taghavi and Miranda (2003) found that non-structural components represent between 65% to 85% of the total initial construction cost. Furthermore, earthquake intensities that trigger damage to non-structural components are typically lower, and in some cases considerably lower, than those required to initiate damage in structural components. Therefore, economic losses in buildings resulting from damage to non-structural components are typically much larger than those associated with structural damage. For example, a detailed evaluation of economic losses in 370 high-rise buildings that were subjected to the 1971 San Fernando earthquake found that the majority of the losses were the result of damage to non-structural components. Among non-structural components, gypsum wallboard partitions represent an important contribution to the total initial investment in non-structural elements, and they are very sensitive to lateral deformation demands resulting from SDR demands in buildings. Whitman et al. (1973) reported that repair costs associated with interior partitions and finishes represented 90% and 65%, respectively, of the total building repair costs in buildings located in intensity zones VI and VII. They concluded that improving the seismic performance of interior partitions would be one of the most effective ways to reduce seismic losses in buildings.

In addition to economic losses, partitions have important environmental impacts when earthquakes occur since partitions are an important fraction of the construction and demolition (C&D) debris which drastically increases after an earthquake. For instance in the city of Los Angeles, C&D debris increased from 150 to 10,000 tons per day following the 1994 Northridge earthquake, strongly affecting landfills and recycling centers (EPA 2008). Moreover, the large volume of damaged partitions that needs to be repaired or replaced leads to increased use of resources and CO₂ emissions.

In order to estimate seismic damage in interior gypsum partition walls, the authors assembled experimental testing results of partitions since 1966 and developed the fragility functions shown in Fig. 1.1. Here damage state 1 (DS1) consists of minor damage that can be repaired by patching, re-taping, sanding and painting the gypsum wallboard. Damage state 2 (DS2) consists of severe cracking, crushing or out of plane buckling of the gypsum wallboards requiring replacement of the gypsum wallboards (without replacing the framing), and damage state 3 (DS3) represents severe damage to the partitions consisting of severe damage to the gypsum wallboards, the screws connecting them to the studs and tracks as well as damage to the steel framing such that replacement of the partition becomes necessary. The same figure shows that for a SDR of 0.5% (i.e., one fourth of those allowed by seismic provisions in the U.S. for steel moment-resisting frame buildings), the probabilities of being in or exceeding DS1 and DS2 are 93% and 15%, respectively. When the SDR is increased to 1.0%, the probabilities of being in or exceeding damage states are 100% for DS1, 81% for DS2 and 17% for DS3, highlighting the poor seismic performance of partitions at levels of SDR that can be easily reached in buildings in moderate level earthquakes.

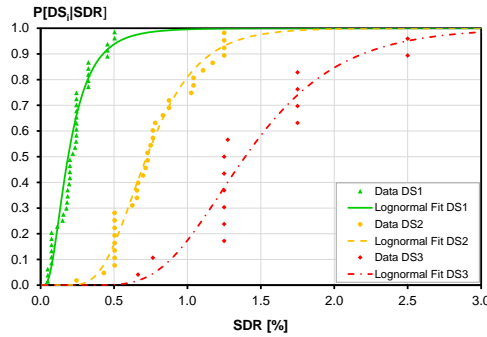


Figure 1.1. Experimental data collected and fragility functions developed for gypsum partition walls.

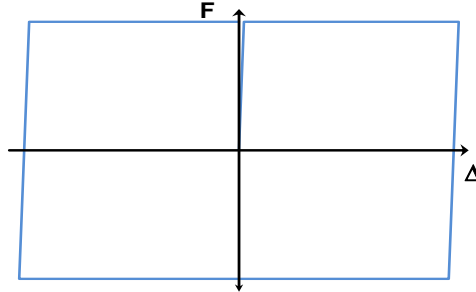


Figure 1.2. Hysteretic model desired for gypsum partition walls.

The goal of this research was to improve the seismic performance of interior gypsum partitions and in particular to increase the SDR level at which damage requiring repairs occurs. The main strategy is to try to isolate the partition from the lateral deformations experienced by the structure. However, in most cases simply disconnecting the upper end of the interior partitions from the floor system of the floor above (so they are in cantilever) is not possible as the partitions also need to resist out-of-plane inertia forces produced by floor accelerations. These inertia forces are important because not only are the gypsum wallboards relatively heavy construction materials but often bookcases and other types of building contents are attached to building partitions. In order to achieve both goals (to isolate the partition from lateral deformations while at the same time providing some resistance to in-plane and out-of-plane inertia forces), a sliding/frictional connection was developed. As illustrated in Fig. 1.2. the interior partition can be relatively rigid but if a certain level of deformation is exceeded, the connection will slide preventing further deformation from being imposed on the partition. Another important constraint for the new connection was that it needed to be done for very little added cost and only with minimal modifications to current construction practices.

2. EXPERIMENTAL TEST PROGRAM

2.1. Basic concepts of the connection

As seen in Fig. 2.1., the connection developed herein consists of a thin (e.g., 5 mm) steel plate which is introduced between the beam or slab of the upper floor and the upper cold-formed steel track of the partition. This plate is attached the slab/beam using conventional fasteners prior to the construction of the interior partition. The upper cold-formed steel track of the partition is not directly attached to the slab/beam, but rather is just “sandwiched” between the thin steel plate and square or rectangular short (e.g., 30 cm) steel tubes (e.g., 25.4 mm by 25.4 mm or 19mm wide by 25.4 mm tall). The short steel

tubes are attached to the thin steel plate by two fasteners, one on each end of the tube. The upper track has large circular holes with diameters equivalent to the track's width (e.g., 88.9 mm) that are centered around two fasteners that attach the short steel tube to the steel plate. These holes accommodate the relative deformations between the upper end of the partition and the floor above the partition. The upper track can be either a vertically slotted track to accommodate vertical deformations caused by live loads in the floor system or a non-slotted track. The slip force on each tube (the lateral force required to initiate sliding) is controlled by the level of axial force introduced by the fasteners connecting the short steel tubes to the thin steel plate. The upper track is then pressed with a nominal normal force between the thin steel plate and the short segments of steel tubing. In the prototype connections the level of axial force was controlled by using commercially available ("off-the-shelf") deformable spring washers, which were selected to achieve a certain nominal slip load. The number of and spacing between connections is selected based on the desired slip force.

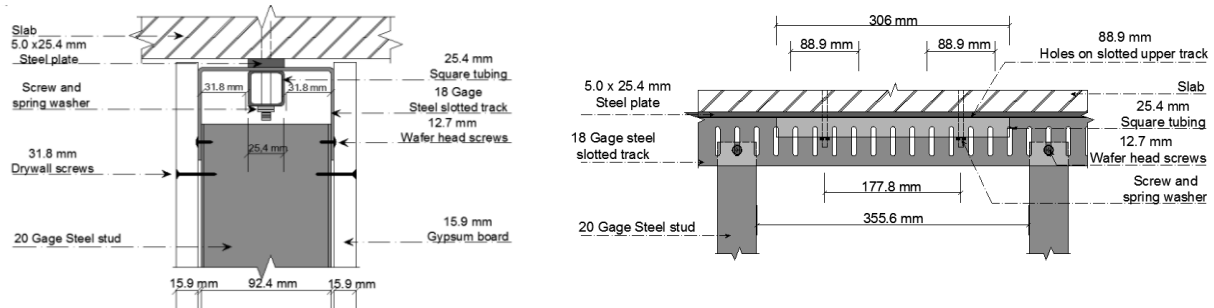


Figure 2.1. Cross section (on the left) and side-view elevation (on the right) of the proposed new sliding/frictional connection.

2.2. Connection specimens and testing

A series of connections were built and tested in order to evaluate constructability aspects of the connection (cost and ease of construction) and performance under cyclic loading. Of particular interest was to determine to what extent the slip force could be controlled and maintained as well as variability of this slip force from connection to connection. Prototype connections were designed for a slip force of 1.33 kN (300 lbf) per connection. The fasteners used to introduce the normal force consisted of two 6 mm cap screws.

Three connection specimens were built and tested with sliding occurring in the longitudinal direction, as shown Fig. 2.2. The cyclic loading protocol consisted of ten increasing steps of lateral displacements, with three cycles applied at each step, until reaching a maximum deformation of 29 mm, which is slightly smaller than the 31.8 mm deformation at which the cap screws would come into contact with the edge of the 88.9 mm circular holes in the steel tracks (assuming the cap screws are completely centered in the circular holes). The loading protocol is shown in Fig. 2.3.



Figure 2.2. Connection specimens testing set up showing the loading direction.

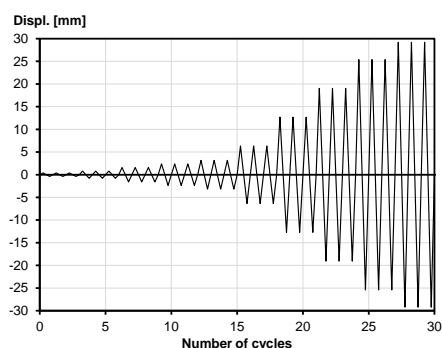


Figure 2.3. Loading protocol used for testing the connection specimens.

Mean sliding forces in connection specimens 1, 2 and 3 were 1.59 kN (358 lbf), 1.58 kN (355 lbf) and 1.25 kN (280 lbf), respectively, which are within 20% of the nominal value. This result is very good considering that the normal force is only calibrated by closing the spring washers. In all three cases the hysteretic behavior was very stable as shown in Fig. 2.4., which shows the hysteretic behavior obtained for connection specimens 1 and 3.

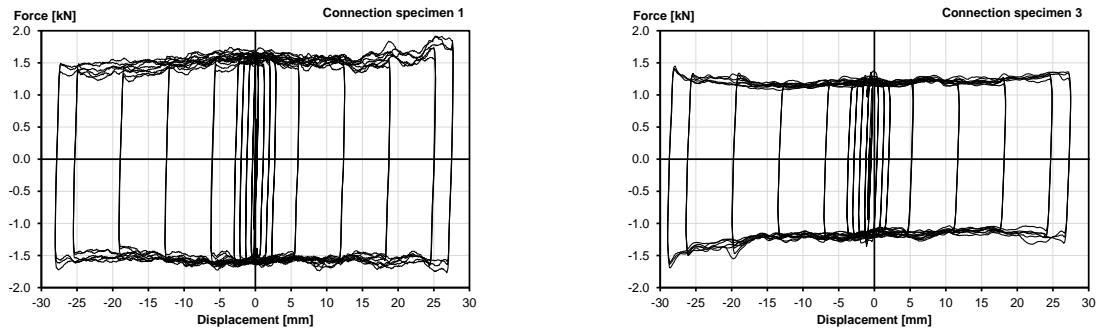


Figure 2.4. Hysteretic behavior for connection specimens 1 (on the left) and 3 (on the right).

2.3. Wall specimens and testing

Once the connection specimens were tested, two full scale partition specimens were built and tested at the structures laboratory of Stanford University's John A. Blume Earthquake Engineering Center. These wall specimens were I-shaped gypsum wallboard partitions consisting of a main wall of 2.4 m (8 ft) by 2.4 m (8 ft) connected to two return walls of 1.2 m (4 ft) by 2.4 m (8 ft) as shown in Figure 2.5. The first specimen was a conventional partition (wall specimen A), whereas the second specimen (wall specimen B) consisted of partitions with two new sliding/frictional connections in the main wall (central) and one connection in each return wall, corresponding to one connection every 1.2 m (4 ft). The plan and elevation of the experimental set up as shown in Fig. 2.6.



Figure 2.5. Wall specimens. On the left, isometric and on the right, actual set up showing the loading direction.

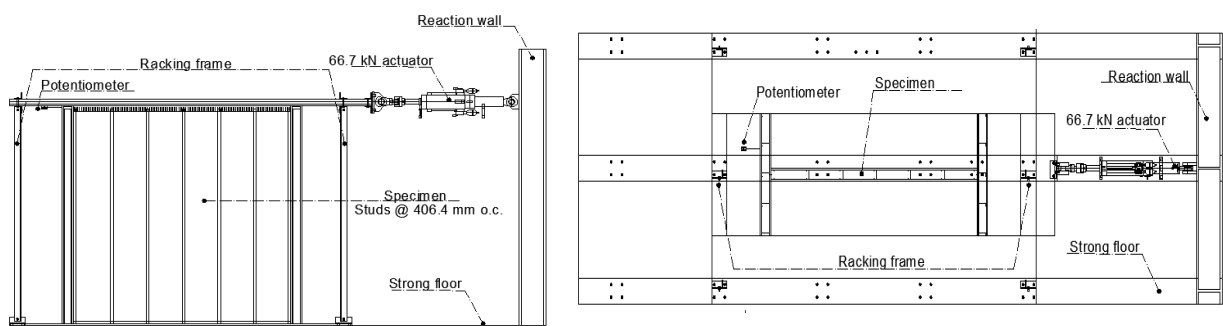


Figure 2.6. Wall specimens set up. Elevation on the left, and plan on the right.

The wall specimens were built using 20 gage cold-formed steel studs spaced 406.4 mm (16 in.) on center attached to 18 gage steel slotted upper tracks and (non-slotted) lower tracks by 12.7 mm (1/2 in.) wafer head screws. Gypsum wallboard panels with a thickness of 15.9 mm (5/8 in.) were attached to the steel frame with 31.8 mm (1-1/4 in.) coarse threaded drywall screws spaced 203.2 mm (8 in.) on center. Generic joint compound and 50.8 mm (2 in.) tape were used on the panel joints and corners between the main wall and the return walls. Finally, the wall specimens were painted with white paint mimicking real construction projects. A potentiometer was installed underneath the slab and attached to the wall specimens in order to measure the relative displacement between the slab and the wall specimens.

The two wall specimens were tested using a quasi-static cyclic testing loading protocol (ATC 2007). A maximum lateral displacement of 101.6 mm (4 in.) and 16 increasing steps were used. In this loading protocol the amplitude a_{i+1} of the step $i + 1$ is given by the following Eqn. 2.1.

$$a_{i+1} = 1.4a_i \quad (2.1)$$

Each step was applied for three cycles, and dividing each step by the height of the specimen (2.4 m), we obtained the loading protocol in terms of SDR shown in Fig. 2.7.

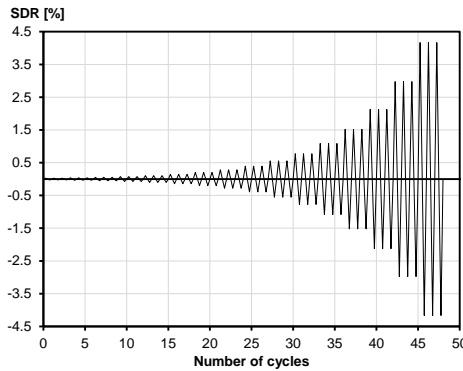


Figure 2.7. Loading protocol used for testing wall specimens.

2.3.1. Wall specimen A-conventional

As seen in Fig. 2.8. (on the left), wall specimen A (conventional construction) experienced significant stiffness degradation and pinching. The first visible damage requiring minor repairs occurred at a SDR of 0.10% when a small crack appeared at one intersection between the main wall and one of the return walls. Damage state 2 occurred at a SDR of 1.08% when a gypsum wallboard from a return wall cracked severely. Finally, DS3 was observed at a SDR of 2.13% when severe crushing of the gypsum boards all over the specimen and buckling of the metal studs in the return walls occurred.

2.3.2. Wall specimen B-with new sliding connections

Fig. 2.8. (on the right) shows the force-SDR relationship for wall specimen B which incorporated the new sliding/frictional connections. The mean sliding force in the specimen was 7.11 kN (1.6 kipf), which is approximately 20% larger than the design value. Stable hysteretic behavior was observed up to a SDR of 1.325%, which corresponds to the lateral deformation at which the square steel tubes in the wall returns came in contact with the upper track. Using a 19 mm wide rectangular tube, this sliding interstory deformation prior to contact can be increased to 35 mm, which for interstory heights commonly used in commercial buildings corresponds to a SDR of about 1%. The maximum lateral force obtained was 23.0 kN, which is very similar to the maximum obtained for wall specimen A. The specimen was able to undergo SDRs up to 1.52% without any damage. The first and second damage state were observed at 2.13% while damage requiring replacement of the partitions (DS3) was not observed until 2.98%.

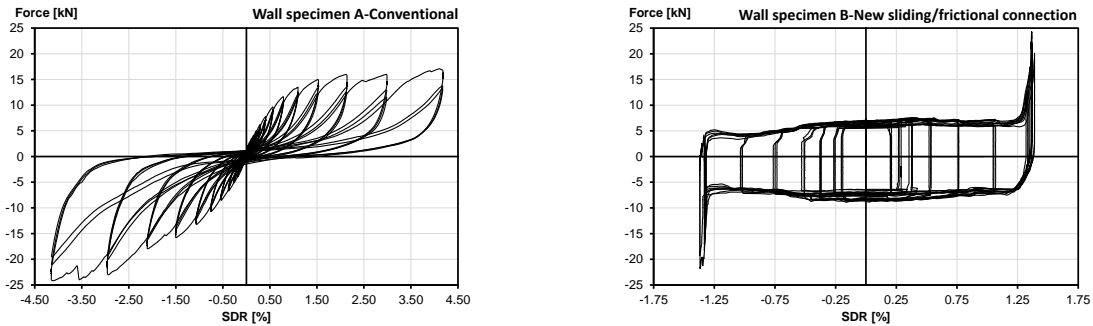


Figure 2.8. Hysteretic behavior for wall specimen A-conventional (on the left) and wall specimen B-new sliding/frictional connection (on the right).

2.3.3. Comparison of performance between wall specimens

In order to illustrate the difference in seismic performance of the two wall specimens, Fig. 2.9. and Fig. 2.10. show the damage state at the intersection between the main wall and one return wall (where damage is concentrated) at 1.52% SDR for both wall specimens. Wall specimen A clearly evidences DS2 (gypsum board crushing and separation between the main wall and the return wall), which is consistent with Fig 1.1., which shows that for 1.52% SDR, the probability of being in or exceeding DS2 is 96%. Wall specimen B is damage free for at the same SDR, which is also consistent with Fig 1.1. considering that wall specimen B is 1.32% SDR isolated from the structure, and consequently the specimen is only taking 0.20% of SDR. For this 0.20% SDR, Fig 1.1. shows a 45% chance of being damage free. Additionally, Table 2.1. summarizes the relationship between the SDRs and the onset of different damage states for wall specimens A and B.



Figure 2.9. Wall specimen A in damage state 2 at 1.52% SDR.

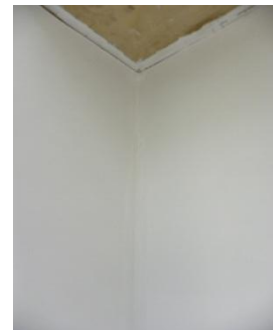


Figure 2.10. Wall specimen B is damage free at 1.52% SDR.

Table 2.1. SDR associated with the onset of each damage state for Wall Specimen A and B.

Damage State	Wall Specimen A. SDR [%]	Wall Specimen B. SDR [%]
DS1	0.10	2.13
DS2	1.08	2.13
DS3	2.13	2.98

3. EFFECTIVENESS OF THE CONNECTION

The performance-based earthquake engineering framework developed by the Pacific Earthquake Engineering Research (PEER) Center measures performance in terms of three decision variables (DV): economic loss, downtime and casualties (Deierlein 2004). However, in addition to economic losses, there is also an important seismic-environmental impact coming from partitions. Therefore, the improved seismic performance of partitions implemented with the new connection will be evaluated by the effectiveness in reducing two DV: seismic-economic losses and seismic-environmental impact for a case study office building located in Los Angeles, California, using the PEER framework.

3.1. Site and seismic hazard curve

The site of the building is the Bulk Mail Center in the city of Los Angeles in California (33.996° N, -118.162° W), characterized by high seismicity and not dominated by unusually strong near-fault effect (Haselton et al. 2008).

The spectral acceleration for the fundamental period of vibration of the structure with 5% damping, $S_a(T_1, 5\%)$, is the intensity measure (IM) used herein, and its seismic hazard curve was obtained by performing lineal interpolation in log-log space from the hazard curves obtained from the Java Ground Motion Parameter Calculator from the USGS (2011) for $T_1=1$ s and $T_1=2$ s to give the hazard curve for $T_1=1.33$ s, which is the fundamental period of the structure described in the next section. The values obtained from USGS correspond to the border of NEHRP sites classes B and C, therefore an amplification factor of 1.5 was used to modify the curve for the site class D, which is the soil condition at the site. This can be seen in Fig 3.1., where the abscissae are $S_a(T_1, 5\%)$, and the ordinates represent the mean annual frequency (MAF) of reaching or exceeding a given value of $S_a(T_1, 5\%)$.

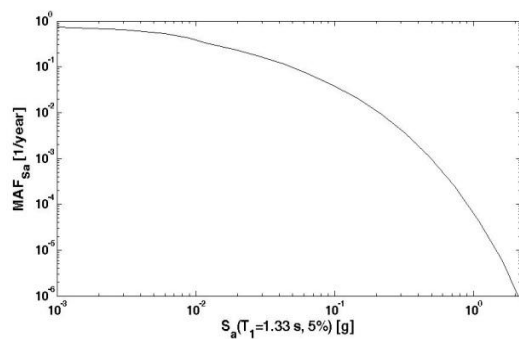


Figure 3.1. Seismic hazard curve.

3.2. Structure, modeling and IDA results

The structure used in this assessment is a four-story steel special moment resisting frame with reduced beam sections designed by Lignos (2008), whose plan and elevation on the axes 1 are shown in Fig 3.2. The lateral resisting system on axes 1 and 4 was designed in accordance with the 2003 International Building Code (ICC 2003) and the 2005 AISC seismic provisions (AISC 2005a, b). The design spectral acceleration ordinates S_{DS} and S_{DI} are 1.0 and 0.6 g, respectively.

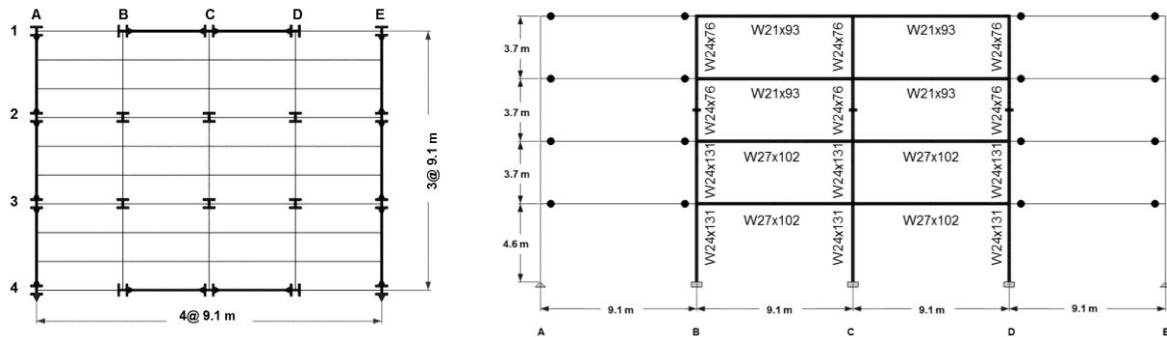


Figure 3.2. Building plan on the left, and elevation on axis 1 on the right.

Eads et al. (2012) modeled the east-west frame on axis 1 using the Open System for Earthquake Engineering Simulation platform (OpenSees 2010) and performed incremental dynamic analyses (IDA) for this structure using a set of 274 ground motions, as shown in Fig. 3.3. These analyses are used in this study. For details of modeling and ground motion selection, the reader is referred to Eads et al. (2012).

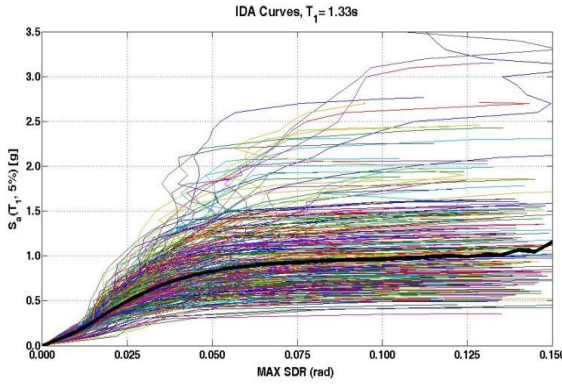


Figure 3.3. Incremental Dynamic Analyses for case-study building.

3.3. Seismic economic loss and seismic environmental impact

The effectiveness in reducing the DV seismic-economic loss and seismic-environmental impact by the use of the new connection was evaluated through the computation of the expected annual loss and expected annual environmental impact on the partitions for two cases: (1) The case study building had 4,475 m² of conventional interior partitions; and (2) The case study building had 4,475 m² of interior partitions having the new sliding/frictional connection.

The first step in this process is the computation of the expected loss and expected environmental impact given that the partitions are in DS1, DS2, and DS3. The expected loss for each DS is the monetary value needed to restore the partitions to their damage-free condition. These values were calculated based on information on RSMeans (2010) and accounting for all the material, labor, fees and profit that a subcontractor would charge, on average, in Los Angeles. Regarding the expected annual environmental impact, several metrics can be assessed, but this study only evaluated the expected annual energy consumption (amount energy used in the extraction, processing, transportation, construction and disposal of each material pro-rated on a yearly basis), sometimes also referred to as embodied energy, and the expected annual global warming potential, GWP, (amount of greenhouse gasses created during the extraction, processing, transportation, construction and disposal of each material pro-rated on a yearly basis) generated to restore the partition walls to the damage free condition from each DS. In order to calculate the energy consumption and the GWP for each DS, life cycle assessment (LCA) was used. LCA is an analytical technique for identifying the resource flow and environmental impacts associated with the provision of products and services (Horne, Grant and Verghese 2009), and this technique was implemented using the software ATHENA ® Impact Estimator for Building (Athena 2011) for the location of Los Angeles. Once the expected value of the DV (loss, energy consumption and GWP) are calculated for each DS, the expected value of these DV given a certain level of SDR and given that the building has not collapsed, can be calculated as shown by Eqn. 3.1

$$E[DV|SDR = sdr, NC] = \sum_{k=1}^{k=3} E[DV|DS_k]P[DS_k|SDR = sdr] \quad (3.1)$$

where $E[DV|SDR = sdr, NC]$ represents the expected value of the decision variable given that the gypsum partitions are undergoing a given SDR equal to sdr (e.g. SDR=1.0%); $E[DV|DS_k]$ represents the expected value of the DV given that the gypsum partitions are in damage state k (e.g. DS1, DS2, or DS3), and $P[DS_k|SDR = sdr]$ represents the probability of being on each damage state k , given that the gypsum partitions are undergoing a given SDR.

It is at this stage where the only difference between conventional and improved partitions (with the new connection) arises because the probabilities of being in each DS for a given SDR are different. Whereas the authors developed fragility functions for conventional partitions, the partition with the

new connection was tested only once, therefore, there are not enough data for its fragility functions. In order to model this, it is assumed that the improved partition will have the same fragilities as the conventional partitions, but shifted due to the sliding between the partitions and the upper slab. As mentioned before, the maximum sliding of the partition in any direction is 31.8 mm, and if a story height of 3.4 m is considered, there is shifting, ϵ , equivalent to 0.94% SDR of sliding between the partitions and the upper slab. This assumption is used in this study, and Fig 3.4. shows the fragilities for conventional and improved partitions.

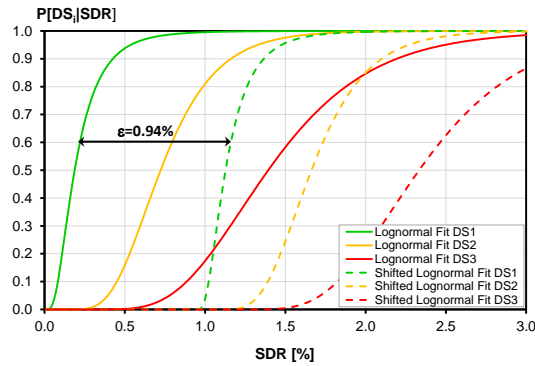


Figure 3.4. Fragility functions for conventional (solid lines) and improved partitions (dashed lines).

The following calculations are the same for conventional and improved partitions. These calculations were performed following the story-based building loss estimation developed by Ramirez (2009).

The expected annual values of the DV economic loss, energy consumption and GWP for both conventional and improved partitions are shown in Table 3.1. As shown in this table, the expected annual loss of conventional partitions is eight times larger than the expected annual loss of the case where interior partitions with improved connections were used. Even larger differences were computed for the environmental impact between conventional and improved partitions.

Table 3.1. Expected annual values of decision variables loss, energy consumption and global warming potential.

Decision Variable (DV)	Conventional Partitions (C)	Improved Partitions (R)	Ratio (C)/(R)
Expected Annual Loss [U.S. dollar/m ² floor]	3.68	0.46	8.00
Expected Annual Energy Consumption [MJ/m ² floor]	21.69	2.29	9.47
Expected Annual Global Warming Potential [kg CO ₂ /m ² floor]	0.34	0.03	11.33

4. CONCLUSIONS

A new sliding/frictional connection for improving the seismic performance of interior gypsum partition walls was developed and tested. Three connection specimens were first tested to verify the performance of the connection under cyclic reversals. A calibrated sliding force of 1.47 kN was obtained, on average, for the connection, which allows the total sliding force to be controlled for any arrangement of partitions by installing an adequate number of connections relative to the length of the interior partition. Then two full-scale specimens were tested. The level of story drift ratio at which the first damage was observed increased drastically from 0.1% for conventional interior partitions to 2.13% for interior partitions that incorporated the new sliding/frictional connection.

In order to evaluate the benefits of incorporating the proposed sliding/frictional connection, expected annual losses and expected annual environmental impact associated with possible damage in conventional interior partition walls in an office building located in Los Angeles were compared to the

results computed for the same building but using interior partitions installed with the proposed sliding/frictional connection. The results showed that the expected annual loss of conventional partitions is eight times larger than the expected annual loss in the building that incorporated the improved partitions, and even larger differences were computed for environmental impact (energy consumption and GWP) between conventional and improved partitions. It is therefore concluded that the proposed connection leads to interior partitions with improved seismic performance that may lead to significant reductions in economic losses and environmental impacts relative to conventional current construction practices for the installation of interior gypsum partitions.

ACKNOWLEDGEMENT

The authors would like to thank the John A. Blume Earthquake Engineering Center of Stanford University, where the experimental testing was conducted. Funding to the first author was provided by Fulbright Chile and Conicyt Chile. This funding is greatly appreciated. Finally, the authors would like to thank Professor Dimitrios Lignos for his help during the construction of the wall specimens and Laura Eads for her careful review and suggestion on this document.

REFERENCES

- ATHENA ® impact estimator for buildings (2011). Version 4.1.14, Athena Institute. Available from: <<http://www.athenasmi.org/tools/impactEstimator/index.html>> (1 March 2011).
- AISC (2005a). Prequalified connections for special and intermediate steel moment frames for seismic applications, AISC 358-05. American Institute of Steel Construction (AISC), Chicago, IL.
- AISC (2005b). Seismic provisions for structural steel buildings, including Supplement No. 1. American Institute of Steel Construction (AISC), Chicago, IL.
- Applied Technology Council (ATC). (2007). Interim testing protocols for determining the seismic performance characteristic of structural and nonstructural components. *FEMA 461*, Federal Emergency Management Agency (FEMA), Washington, DC.
- Balboni, B. (ed.). (2010). RS Means Square Foot Costs 2011, R.S. Means Company, Kingston, MA.
- Deierlein, G.G. (2004). Overview of a comprehensive framework for earthquake performance assessment. In *International Workshop on Performance-Based Seismic Design – Concepts and Implementation*, Bled S, Fajfar P, Krawinkler H (eds). PEER 2004/05: Berkeley, CA, 2004; 15–26.
- Eads, L., Miranda, E., Krawinkler, H. and Lignos, D.G. (2012). An efficient method for estimating the collapse risk of structures in seismic regions. *Earthquake Engineering & Structural Dynamics*, DOI: 10.1002/eqe.2191 (in print).
- Haselton, C.B., Goulet, C.A., Mitrani-Reiser, J., Beck, J.L., Deierlein, G.G., Porter, K.A., Stewart, J.P. and Taciroglu, E. (2008). An assessment to benchmark the seismic performance of a code-conforming reinforced concrete moment-frame building. *PEER Report 2007/12*, Pacific Earthquake Engineering Research Center (PEER), University of California, Berkeley, CA.
- Horne, R., Grant, T. and Verghese, K. (2009). Life cycle assessment: Principles, practice and prospects, CSIRO, Collingwood, Australia.
- International Code Council (ICC). (2003). International Building Code. ICC, Falls Church, VA.
- Java Ground Motion Parameter Calculator (2011). Version 5.1.0, United States Geological Survey (USGS). <<http://earthquake.usgs.gov/hazards/designmaps/javacalc.php>> (1 July 2011).
- Lignos, D.G. (2008). Sidesway collapse of deteriorating structural systems under seismic excitations. *Ph.D. Thesis*, Department of Civil and Environmental Engineering, Stanford University, Stanford, CA.
- Open System for Earthquake Engineering Simulation (OpenSees) (2009). Version 2.1.1, Pacific Earthquake Engineering Research Center (PEER). <<http://opensees.berkeley.edu>> (6 June 2010).
- Ramirez, C. (2009). Building-specific loss estimation methods and tools for simplified performance-based earthquake engineering. *Ph.D. Thesis*, Department of Civil and Environmental Engineering, Stanford University, Stanford, CA.
- Taghavi, S. and Miranda, E. (2003). Response assessment of nonstructural building elements. *PEER Report 2003/05*, Pacific Earthquake Engineering Research Center (PEER), University of California, Berkeley, CA.
- EPA (2008). Planning for natural disaster debris. U.S. Environmental Protection Agency.
- USGS (2011). Mineral Commodity Summaries 2001. U.S. Geological Service.
- Whitman, R., Hong, S. and Reed, J. (1973). Damage statistic for high-rise buildings in the vicinity of the San Fernando earthquake. *Optimum seismic protection and building damage statistics report no. 7*, Department of Civil Engineering, MIT, Cambridge, MA.